https://africanjournalofbiomedicalresearch.com/index.php/AJBR
Afr. J. Biomed. Res. Vol. 27(3) (December 2024); 2822-2832

Research Article

Antimicrobial activity of Diisooctyl phthalate fraction from endophytic fungus *Hypoxylon griseobrunneum* isolated from *Thunbergia fragrans*

M.S Mangalagowri[1] and Krishna K[2*]

[1]Research Scholar, Department of Botany, Yuvaraja's College, University of Mysore, Mysuru, Karnataka, India. msgowri.drs@gmail.com
[2*]Professor, Department of Botany, Yuvaraja's College, University of Mysore, Mysuru, Karnataka, India. drkkuppi@gmail.com

***Corresponding Author:** Dr. K. Krishna
*Professor, Yuvaraja's College, University of Mysore, Mysuru-570005, Email: msgowri.drs@gmail.com

Abstract
The present study investigated the isolation, characterization, and antimicrobial potential of endophytic fungi from the medicinal plant *Thunbergia fragrans*. Six fungal isolates were obtained from surface-sterilized stems and leaves. Among these, isolated TF3 demonstrated the strongest antimicrobial activity. Ethyl acetate extract of TF3 showed significant inhibition against *Bacillus subtilis*, *Pseudomonas aeruginosa*, *Staphylococcus aureus* and *Escherichia coli* with inhibition zones ranging from 20 ± 0.54 to 23 ± 0.89 mm, occasionally exceeding those of gentamicin. Minimum inhibitory concentration (MIC) values ranged from 5 to 10 mg/ml, with *E. coli* showing the lowest MIC (5 ± 0.18 mg/ml). The extract also exhibited antifungal activity against *C. albicans* (12 ± 0.31 mm), *Aspergillus fumigatus* (11 ± 0.28 mm), *Fusarium oxysporum* (10 ± 0.22 mm) and *Penicillium chrysogenum* (10 ± 0.17 mm), with MIC and minimum fungicidal concentrations (MFC) of 10 mg/ml. Molecular identification via ITS rDNA sequencing identified TF3 as *Hypoxylon griseobrunneum* (GenBank accession: PP794700). Column chromatography was used to partially purify the methanol fraction, which was analyzed by GC-MS, revealing six major compounds, predominantly diisooctyl phthalate (DIOP). The structure of DIOP was further confirmed by FT-IR and ^{1}H-NMR spectroscopy. This is the first report of antimicrobial activity from a partially purified fraction containing DIOP from *H. griseobrunneum* isolated from *T. fragrans*. The findings underscore the potential of endophytic fungi from medicinal plants as promising sources of natural antimicrobial agents.

Keywords: Endophytic fungi ,*Hypoxylon griseobrunneum* ,Antimicrobial activity ,Diisooctyl phthalate ,*Thunbergia fragrans.*

Author of correspondence: Email: msgowri.drs@gmail.com

Received :26/09/2024 Acceptance :12/12/2024

DOI: https://doi.org/10.53555/AJBR.v27i3.7369

© 2024 The Author(s).
This article has been published under the terms of Creative Commons Attribution-Noncommercial 4.0 International License (CC BY-NC 4.0), which permits noncommercial unrestricted use, distribution, and reproduction in any medium, provided that the following statement is provided. "This article has been published in the African Journal of Biomedical Research"

Introduction

The medicinal value of plants is widely recognized, and endophytes- microorganisms that reside within plant tissues-hold significant promise in the development of novel therapeutics. The term "endophyte," coined by the German scientist Heinrich Anton de Bary in 1884,

refers to fungi or bacteria that colonize plant tissues without causing visible symptoms in their host (Wilson, 1995). The interaction between endophytic fungi and their host plants is characterized by mutualistic symbiosis, where both parties benefit. Plants provide shelter and nutrients, while endophytes produce secondary metabolites that enhance plant survival under various abiotic and biotic stresses (Faeth *et al.,* 2002).Endophytes are known to synthesize a diverse array of metabolites, including alkaloids, terpenoids, steroids, quinones, isocoumarins, flavonoids, phenolic acids, and peptides. Some species have been found to produce novel antimicrobial agents, such as Cryptocandin from *Cryptosporiopsis quercina*, and potent anticancer compounds like Taxol from *Taxomyces andreanae*. Others produce industrially valuable compounds such as enzymes and solvents (Strobel *et al*., 2004). Approximately 80% of endophytic fungi produce secondary metabolites with biological activity, exhibiting fungicidal, antibacterial, and herbicidal properties (Schulz *et al.,* 2002). The growing demand for natural products in agriculture, medicine, and industry has shifted attention toward endophytic microorganisms as promising sources of new bioactive compounds.*Thunbergia fragrans* commonly known as **"**white lady**"** or "whitethroat," is a fast-growing perennial climbing vine native to tropical Asia and widely naturalized in other regions. It has a long history of use in traditional medicine systems, where its leaves, flowers, and stems are utilized to treat ailments such as fever, respiratory infections, skin diseases, and inflammation. Pharmacological studies have confirmed that *T. fragrans* exhibits anti-inflammatory, analgesic, antipyretic, antioxidant, and antimicrobial activities. Phytochemical investigations reveal the presence of flavonoids, alkaloids, tannins, phenolic compounds, and essential oils, all contributing to its therapeutic efficacy. Given its rich phytochemistry and medicinal relevance, *T. fragrans* is an ideal candidate for endophytic fungal isolation, as these fungi may produce novel bioactive metabolites that mimic or complement the host plant's medicinal properties.This study aims to isolate the endophytic fungus *Hypoxylon griseobrunneum* from *Thunbergia fragrans* and evaluate its molecular characterization and antimicrobial potential. The chemical characterization of its bioactive metabolites was carried out using Gas Chromatography-Mass Spectrometry (GC-MS), Fourier Transform Infrared (FT-IR) spectroscopy, and Nuclear Magnetic Resonance (^1H NMR) analysis, showcasing the untapped potential of endophytes for pharmaceutical applications.

Materials and methods

Collection of plant samples

Healthy, mature, and fresh *Thunbergia fragrans* (Acanthaceae) plant samples were collected from Mysore, Karnataka,India (12° 18′ 26″ N latitude and 76° 38′ 59″ E). The leaves and stems were cut from the field-collected plants, immediately placed in sterile polythene bags, and transported to the laboratory. Upon arrival, the samples were stored under appropriate conditions for further analysis (Singh *et al*., 2021). Prior to surface sterilization, the plant materials were thoroughly washed 2-3 times with running tap water. The taxonomic identification of the plant species was confirmed by the Botanical Survey of India (BSI), Coimbatore, Tamil Nadu.

Isolation of the endophytic fungi from *T. fragrans*

The isolation of endophytic fungi was performed following the method described by (Giang *et al*., 2021). Surface sterilization of the plant tissues was carried out by immersing them in 70% ethanol for a few minutes, followed by soaking in a 1-2% sodium hypochlorite (NaOCl) solution for 2-5 minutes. The tissues were then washed in 70% ethanol for 1 minute and rinsed three times with sterile distilled water before being dried on sterile blotting paper. Using sterile blades, the leaves and stemwere cut into small segments. These segments were plated onto Potato Dextrose Agar (PDA) enriched with 100 mg/mL tetracycline to inhibit bacterial growth. To ensure the effectiveness of the sterilization process, aliquots of the final rinse water were also plated on PDA. The plates were sealed with parafilm and incubated at 28°C for 7-14 days to allow fungal growth. After this incubation period, fungal mycelial growth emerged from the plant segments. The emerging fungal colonies were subcultured onto fresh plates to obtain pure cultures for further analysis . The pure fungal strains were photographed and preserved on PDA slants at -80°C for future use.

Morphological and molecular identification of fungal isolates

Morphological identification

Fungal isolates were grown on Potato Dextrose Agar (PDA) and incubated at 28 ± 2 °C for 7 days. Colony morphology was recorded based on characteristics such as color, texture, margin, pigmentation, and surface structure. For microscopic observation, a small portion of fungal mycelium was mounted on a clean glass slide with a drop of lactophenol cotton blue stain and covered with a coverslip. Slides were observed under a compound light microscope at 40× magnification to examine features such as hyphal structure, conidiophores, and conidia. Tentative identification was carried out using standard mycological keys and taxonomic manuals.

Molecular identification (ITS rDNA Sequencing) Morphologically distinct isolates were selected for molecular identification. Genomic DNA was extracted using the CTAB method, and DNA quality was assessed using 1.0% agarose gel electrophoresis. The

Internal Transcribed Spacer (ITS) region of rDNA was amplified using universal primers ITS1 (5′-TCCGTAGGTGAACCTGCGG-3′) and ITS4 (5′-TCCTCCGCTTATTGATATGC-3′) following the protocol described by White *et al.* (1990). PCR conditions included an initial denaturation at 94 °C for 5 minutes, followed by 35 cycles of denaturation at 94 °C for 30 seconds, annealing at 55 °C for 30 seconds, and extension at 72 °C for 1 minute, with a final extension at 72 °C for 10 minutes. PCR products (~600 bp) were confirmed by agarose gel electrophoresis and purified using a PCR cleanup kit. Bidirectional sequencing was performed using an ABI 3730xl Genetic Analyzer. The obtained sequences were assembled and analyzed using the NCBI BLAST tool to identify species-level similarity. Sequences were submitted to GenBank, and accession numbers were obtained.

Phylogenetic analysis

The ITS sequence of the most active isolate was aligned with closely related fungal sequences retrieved from NCBI using ClustalW in MEGA version 11 (Tamura, Stecher, & Kumar, 2021). Phylogenetic analysis was performed using the Neighbor-Joining (NJ) method. Bootstrap analysis with 1000 replicates was conducted to assess the reliability of the tree topology. The phylogenetic tree was visualized and edited in MEGA 11.

Secondary metabolites extraction

The secondary metabolites were extracted and modified as necessary during the process described by Rodrigues *et al*., (2000). Fungal cultures were grown in 150 mL of potato dextrose broth (PDB) in 250 mL Erlenmeyer flasks, which were autoclaved prior to inoculation. The cultures were incubated under stationary state at room temperature for 18–21 days. After the incubation period, the culture broth was filtered through muslin cloth, followed by filtration using Whatman filter paper to separate the mycelium. The filtrate was then mixed with ethyl acetate (150 mL ethyl acetate per 100 mL of filtrate), agitated thoroughly, and left at room temperature for 2 hours. The organic phase was separated using a separating funnel and evaporated, yielding a dry residue. This residue was dissolved in DMSO for further analysis, and the extract was stored at 4–5°C.

Antimicrobial activity of secondary metabolites

The antimicrobial activity of the fungal extract was evaluated using the agar well diffusion method with slight modifications (Brantner *et al.,* 1994; Magaldi *et al.,* 2004). For antibacterial testing, nutrient agar was prepared and sterilized by autoclaving at 121 °C for 15 minutes. After cooling to 45–50 °C, 25 mL of the sterile medium was poured into sterile Petri dishes and allowed to solidify under aseptic conditions. Fresh cultures of selected bacterial strains Gram-positive *Staphylococcus aureus* (MTCC 96) and *Bacillus subtilis* (168), and Gram-negative *Escherichia coli* (MTCC 118) and *Pseudomonas aeruginosa* (MTCC 424) were uniformly spread on the surface of the agar using sterile cotton swabs. Wells of 4 mm diameter were aseptically punched into the agar using a sterile cork borer. Each well was filled with 100 µL of fungal extract (50 mg/mL in DMSO). Gentamicin (1 mg/mL in DMSO) served as positive control, while pure DMSO was used as negative control. The plates were incubated at 37 °C for 24 hours, after which zones of inhibition (ZOI) were measured in millimeters using a vernier caliper.

For antifungal testing, fresh fungal cultures*Candida albicans* ATCC 90028, *Aspergillus fumigatus* MTCC 9657, *Fusarium oxysporum* MTCC 1755, and *Penicillium chrysogenum* MTCC 108 were uniformly spread on potato dextrose agar (PDA) plates. Wells were aseptically punched and filled with 100 µL of fungal extract (10 mg/mL in DMSO). Fluconazole (1 mg/mL) was used as positive control. The plates were incubated at 30 °C for 2–3 days, and inhibition zones were measured inmillimeters.

Determination of MIC for antimicrobial activity of TF3 extract

The Minimum Inhibitory Concentration (MIC), Minimum Bactericidal Concentration (MBC), and IC_{50} of the extract against selected pathogens were determined for both bacteria and fungi using the broth dilution method. For bacterial pathogens (*E. coli* MTCC118, *Pseudomonas aeruginosa* MTCC424, *Bacillus subtilis* 168, and *Staphylococcus aureus* MTCC96), overnight cultures were suspended in nutrient broth, and turbidity was adjusted to 0.5 McFarland, yielding a suspension of approximately 10^8 CFU/mL. A two-fold dilution of the extract was added to a 96-well microtiter plate, followed by the addition of the bacterial suspension, and the plate was incubated at 37°C for 24 hours. The MIC was the lowest concentration showing no visible growth, and the MBC was determined by transferring non-turbid samples to agar plates and assessing growth after incubation at 37°C for 24-48hours.

For fungal pathogens (*Candida albicans* ATCC 0028, *Aspergillus fumigatus* MTCC 9657, *Fusarium oxysporum* MTCC 1755, and *Penicillium chrysogenum* MTCC 5108), fungal suspensions of 1 × 10^6 spores/mL in Potato Dextrose Broth (PDB) were used, with the same two-fold dilution process followed by the addition of the spore suspension to the microtiter plate. Incubation was carried out at 30°C for 2 days to determine the MIC, defined as the lowest concentration with no visible fungal growth. The MFC was determined by transferring non-turbid wells to agar plates and assessing growth after 2-3 days of incubation at 30°C. For both bacterial and fungal tests,

IC_{50} values were determined by measuring the optical density (OD) at 600 nm after incubation and calculating the percentage reduction in absorbance compared to controls, which reflects the concentration required to inhibit 50% of microbial growth.

Column chromatography of ethyl acetate extract of TF3

Column chromatography was performed using a cylindrical glass column (1.5 × 22 cm), which was firmly secured to a chromatography stand and pre-packed with silica gel. A sample solution (50 mg/mL) of the TF3 ethyl acetate extract was carefully loaded onto the top of the silica column. Elution was carried out under gravity using solvents of increasing polarity *n*-hexane, ethyl acetate, and methanol passed sequentially through the column at a uniform flow rate. Each fraction was collected separately in clean, labeled test tubes and numbered consecutively for further analysis.The collected fractions were concentrated and stored at 4 °C for further phytochemical screening and antimicrobial analysis (Mahabaleshwara *et al*., 2016).

Antibacterial activity of secondary metabolite fractions of TF3 extract

The hexane, ethyl acetate, and methanol fractions of the TF3 extract were dried and re-dissolved in dimethyl sulfoxide (DMSO) for antibacterial testing. The activity was evaluated against *Bacillus subtilis* using the well diffusion assay, as previously described.

GC-MS analysis of TF3 methanol fraction

Gas Chromatography–Mass Spectrometry (GC-MS) analysis was performed using a Clarus 680 GC system equipped with a fused silica HP-5MS capillary column (5% biphenyl, 95% dimethylpolysiloxane; 30 m × 0.25 mm i.d. × 0.25 µm film thickness). Helium was used as the carrier gas at a constant flow rate of 2 mL/min. The injector temperature was set at 250 °C, and 0.1 µL of the sample was injected in splitless mode. The oven temperature program was as follows: the initial temperature was set at 100 °C and held for 2 minutes, then increased to 200 °C at a rate of 10 °C/min and held for 1 minute, followed by a ramp to 300 °C at 25 °C/min, where it was held for 8 minutes. Mass spectrometric detection was conducted under electron impact (EI) ionization at 70 eV. The ion source and transfer line temperatures were set at 230 °C and 250 °C, respectively. The scan time was 0.2 seconds with a scan interval of 0.1 seconds. The mass spectra of the eluted compounds were interpreted using the NIST (2017) mass spectral library for compound Identification.

NMR analysis

For NMR analysis of the TF3 methanol fraction, a portion of the fraction (5-10 mg) was dissolved in a suitable deuterated solvent ($CDCl_3$) and transferred to a 5 mm NMR tube. Proton (^1H) NMR spectra were recorded using a high-field NMR spectrometer (400 MHz). The spectra were processed for phasing, baseline correction, and peak integration. The chemical shifts, coupling patterns, and integration data were analyzed to assign proton environments. The obtained NMR data were compared with literature references to confirm the identity of the compounds.

FT-IR Spectroscopy

For FT-IR analysis of the TF3 methanol fraction, a small amount of the fraction (2-5 mg) was placed on an infrared transparent crystal. The sample was subjected to FTATIR spectroscopy using a high-resolution FTATIR spectrometer. The spectrum was recorded over a range of 4000-400 cm^{-1}, with an appropriate number of scans (typically 32) and a resolution of 4 cm^{-1}. The resulting spectrum was analyzed for characteristic functional group vibrations and compared with known reference spectra to identify key molecular features and functional groups present in the TF3 methanol fraction.

Statistical analysis

Mean, standard deviation and descriptive statistics were performed using PRISM software (PRISM 8 Version 8.0.2). Comparison of mean and significance was determined by one-way ANOVA with Geisser-Greenhouse model. Multiple comparison was made using Tukey's test and the significance level was measured with $p<0.05$.

Results

Isolation and Identification of endophytic fungi from *Thunbergia fragrans*

Six endophytic fungal strains were isolated from surface-sterilized leaf and stem tissues of *Thunbergia fragrans*. All isolates showed visible growth on PDA within 3–7 days of incubation at 28 ± 2 °C. The isolates were labeled TF1,TF2, TF3, TF7, TF11, and TF12 and displayed diverse colony morphologies, suggesting a varied endophytic fungal community associated with the plant.

Molecular identification through ITS rRNA gene sequencing confirmed the identities of the isolates, with sequence comparisons in the NCBI database revealing close matches to known species. The isolates were identified as *Talaromyces tratensis* (TF1), *Cladosporium cladosporioides* (TF2), *Hypoxylon griseobrunneum* (TF3), *Meyerozyma caribbica* (TF11), among others (Table 1). The ITS sequences were deposited in GenBank with accession numbers listed.

Based on its distinct morphology and molecular profile, isolate TF3 (*Hypoxylon griseobrunneum*) was selected for further phylogenetic analysis and bioactivity study.

Table 1. Identified endophytic fungal isolates from different parts of *T.fragrans* with accession numbers

Isolated fungus	Plant organ	Accession number
Talaromyces tratensis	Leaf	PQ050373
Cladosporium cladosporioides	Stem	PP794672
Hypoxylon griseobrunneum	Leaf	PP794700
Meyerozyma caribbica	Stem	PQ047836
Penicillium sp.	Leaf	-
Aspergillus sp.	Leaf	-

Antibacterial activity of secondary metabolites:

Extracts of isolated endophytic fungal species were evaluated for anti bacterial activity against both Gram positive and Gram-negative pathogens. The crudeextractof all six fungal strains, dissolved in DMSO, demonstrated antibacterial activity against the tested bacteria, with a few exceptions. Notably, the extract of TF3 exhibited the largest inhibition zones in the well diffusion assay. The strongest activity was observed against *Bacillus subtilis*, with a zone of inhibition measuring 23 ± 0.18mm, followed by *Staphylococcus aureus*, *Escherichia coli*, and *Pseudomonas aeruginosa* (with inhibition zones of 20 ± 0.54mm, 20 ± 0.63 mm, and 22 ± 0.89 mm, respectively). The results from gentamicin, used as a control, showed similar inhibition patterns, with zone diameters of 18 ± 0.09 mm, 18 ± 0.09 mm, 16 ± 0.09 mm, and 18 ± 0.09 mm for *B. subtilis*, *S. aureus*, *E. coli*, and *P. aeruginosa*, respectively (Table 2).

Table:2. Antibacterial activity of secondary metabolites extract

Sample	Zone of inhibition (mm in diameter)			
	E. coli	***P. aeruginosa***	***B. subtilis***	***S. aureus***
TF1	20 ±0.89^{a}	18 ±0.89^{a}	20 ±0.54^{b}	20 ±0.45^{b}
TF3	20 ±0.63^{a}	22 ±0.27^{c}	23 ±0.18^{b}	20 ±0.54^{b}
TF7	22 ±0.45^{b}	20 ±0.45^{b}	22 ±0.45^{c}	22 ±0.89^{c}
TF11	22 ±0.45^{b}	18 ±0.00^{a}	22 ±0.09^{c}	22 ±0.09^{c}
TF12	20 ±0.89^{a}	20 ±0.45^{b}	20 ±0.45^{b}	22 ±0.36^{c}
TF2	20 ±1.43^{a}	22 ±0.54^{c}	22 ±0.54^{c}	20 ±0.45^{b}
Antibiotic	16 ±0.09^{c}	18 ±0.09^{a}	18 ±0.09^{a}	18 ±0.09^{a}

Values are mean ± SD (n=2); Different alphabet in the same column are significantly different ($p<0.05$).

Table 3. MIC, MBC, and IC_{50} values of the ethyl acetate extract of TF-3 against various pathogens were determined

Extract	Pathogens	MIC (mg/ml)	MBC (mg/ml)	IC_{50} (mg/ml)
Ethyl acetate extract of TF-3	*E. coli*	5	10	1.09
	P.aeruginosa	10	10	1.56
	B. subtilis	10	10	1.25
	S. aureus	10	10	1.875

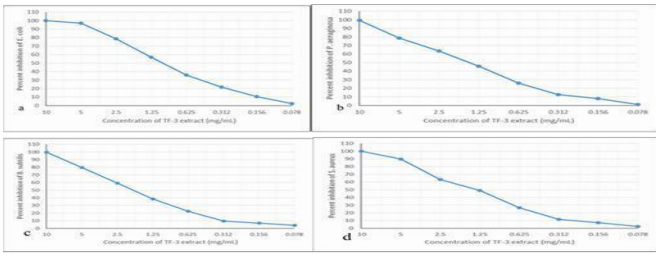


Figure3: Percentage inhibition of(a). *E. coli*, (b)*P.aeruginosa* (c). *B. subtilis* and (d). *S. aureus* with different concentration of Ethyl acetate extract of TF3

Antifungal activity of secondary metabolites:

The ethyl acetate extract of all six fungal isolates was screened for antifungal activity against four pathogenic strains using the agar well diffusion method on PDA plates. The extract from TF3 exhibited the highest activity against *Aspergillus fumigatus*, with an inhibition zone of 12 ± 0.54 mm, followed by *Candida albicans*, *Fusarium oxysporum*, and *Penicillium chrysogenum*, with inhibition zones of 10 ± 0.45 mm each. Fluconazole, used as a comparative control, showed the highest activity against *C. albicans* (24 ± 0.09 mm), followed by *P. chrysogenum*, *A. fumigatus*, and *F. oxysporum* (20 ± 0.09 mm, 18 ± 0.09 mm, and 18 ± 0.18 mm, respectively). In contrast, the extract from other fungal strains failed to show activity against some pathogens (Table 4).

Table 4.Antifungal activity of secondary metabolites extracts

Sample	Zone of inhibition (mm in diameter)			
	C. albicans	*A fumigatus*	*F. oxysporium*	*P. chrysogenum*
TF1	10 ±0.72	12 ±0.36	10 ±0.54	10 ±0.27
TF3	10 ±0.45	12 ±0.54	10 ±0.18	10 ±0.45
TF7	-	-	-	-
TF11	10 ±0.36	-	10 ±0.45	10 ±0.27
TF12	-	12 ±0.18	10 ±0.54	10 ±0.18
TF2	10 ±0.36	-	10 ±0.72	-
Antibiotic	24 ±0.09	18 ±0.09	18 ±0.18	20 ±0.09

Values are mean ± SD (n=2); There was no statistical difference ($p>0.05$) between the sample. However, significant difference ($p<0.05$) was observed with respect to standard antibiotic. (-) no inhibitor

Table 5 MIC, MFC, and IC_{50} values of the ethyl acetate extract of TF-3 were determined for various pathogen s

Pathogens	MIC (mg/ml)	MFC (mg/ml	IC50 (mg/ml)
C. albicans	10	10	2.19
F. oxysporium	10	10	1.87
A. fumigatus	10	10	1.25
P. chrysogenum	10	10	2.5

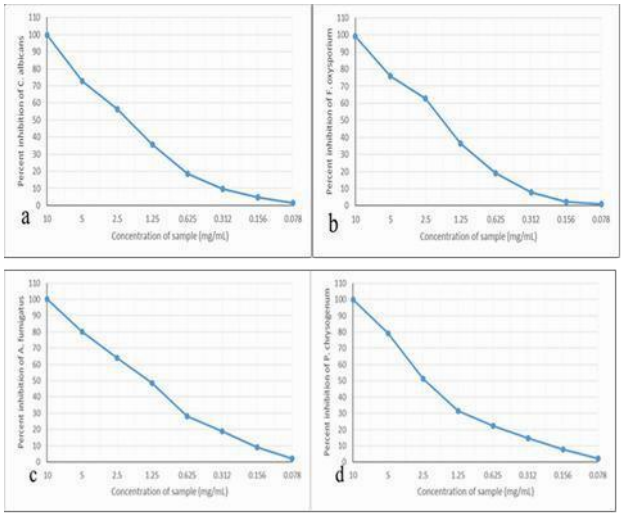


Figure 4: Percentage inhibition of (a) C. albicans, (b) F. oxysporium (c)A. fumigatus, and (d)P. chrysogenum with different concentration of Ethyl acetate extract Of TF3

Characterization of *H. griseobrunneum*TF-3

The pure colony of TF3 morphologically appeared Blackgeryish hair in texture, initially light greyish witha prominent smooth edge, and diffusible black pigmentation in the surrounding medium. The reverseside of the colony exhibited a dark coloration. Microscopic examination revealed septate hyphae with short, smooth conidiophorest terminating in subglobose vesicles. Chains of spherical to sub-spherical conidia were observed, forming dense clusters radiating fromthe vesicle that had Granular Irregular, Raised,andEntire phenotypictraits, including its colony structureand microscopic examination (figure1)**.** The speciesllevel confirmation wasdoneby multiple sequence alignment and phylogenetictree of ITS sequence (Figure 2) which showed 95% similarity with *Hypoxylon griseobrunneum***.** The full-length sequence of the ITS of the current isolate *Hypoxylon griseobrunneum* TF3 is available in the NCBI database under the GenBank accession number PP794700.

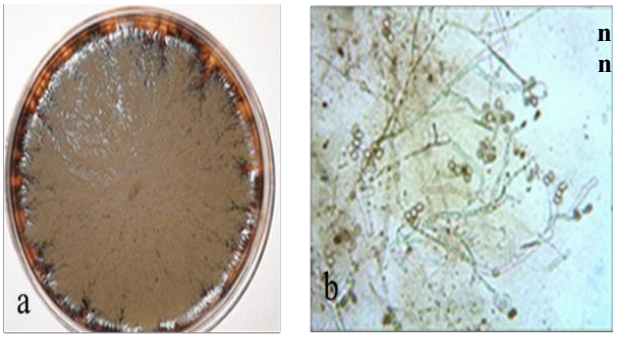


Figure1.Morphological and microscopic observatio of fungal endophytes isolated from *T.fragrans* o PDA plates (a-b) *Hypoxylon griseobrunneum*

Phylogenetic tree of *Hypoxylon griseobrunneum*

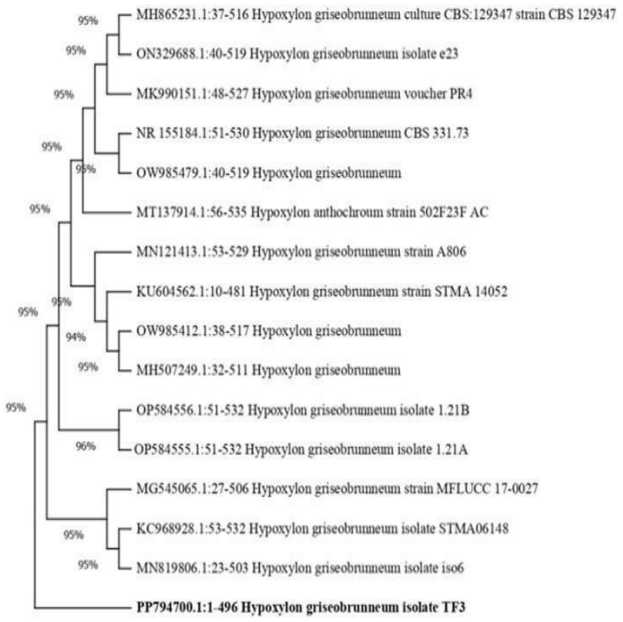


Figure 2. Optimum phylogenetic tree constructed in MEGA -11, by neighbor-joining method and evolutionary distance computed using the maximum composite likelihood method (NJ-MCL) obtained from ITS of TF3 which confirmed to be *Hypoxylon griseobrunneum***.**

Column chromatography of ethyl acetate extract of *Hypoxylon griseobrunneum* (TF3)

Column chromatography of the ethyl acetate extracts from the fungal isolates was carried out using a gradient solvent system (n-hexane → ethyl acetate → methanol). This process enabled the separation of multiple fractions based on polarity. The eluates were collected in sequentially numbered test tubes under gravity flow.

Among the collected fractions, those from *Hypoxylon griseobrunneum* TF3 were selected for biological evaluation based on their solvent systems and presumed bioactive compound content. These fractions were directly subjected to biological assays to assess their potential antimicrobial properties.

Biological activities of fractions

Antibacterial activity of secondary metabolite fractions of *H. griseobrunneum*

The antibacterial activity of fractions from *Hypoxylon griseobrunneum* TF3 extracted using different solvents was evaluated against *Bacillus subtilis* 168 using the well diffusion assay.

The methanol extract of *H.griseobrunneum* TF3 showed the highest activity (11 mm), followed by the ethyl acetate extract (7 mm), while the hexane extract showed no inhibitory effect (0 mm) and Positive control gentamicin 18mm showed in figure 5.

These findings suggest that the methanol fractions of *H.griseobrunneum* TF3 possess stronger antibacterial activity than the ethyl acetate and hexane fractions, indicating that the active antibacterial compounds are more soluble in polar solvents like methanol.

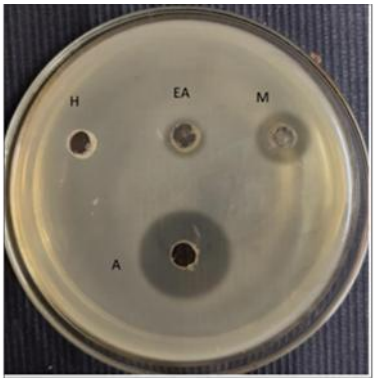


Fig 5. Antimicrobial activity zone of inhibition (mm) shown by column fractions against bacterial strain a. *B. subtilis* 168 .

Selection of methanol fractions of *H. griseobrunneum* for GC-MS analysis

Based on the antibacterial screening, the methanol fractions of *H. griseobrunneum* TF3 exhibited the highest zones of inhibition. This indicates the presence of polar bioactive compounds with antibacterial properties.

GC-MS analysis of the methanol fraction of *H. griseobrunneum* TF3 revealed the presence of six distinct peaks corresponding to various bioactive compounds. These included fatty acid esters, chlorinated benzoic acid hydrazides, long-chain unsaturated fatty acids, and notably, phthalate esters.The major compound detected was Diisooctyl phthalate (RT: 18.961), comprising the highest relative abundance at 1.693% of the total chromatographic area, followed by compounds such as 9,12-Octadecadienoyl chloride**,** 8,11,14-Eicosatrienoic acid, and Cyclopentaneundecanoic acid methyl ester. The compounds detected suggest the presence of a mixture of aliphatic acids and esters, some of which may contribute to the bioactivity of the extract. Table 7 summarizes the identified compounds, their retention times, molecular formulas, peak areas, and area percentages.

Table: 7 GC-MS detected compounds in the methanol fraction of *Hypoxylon griseobrunneum* TF3 extract

Peak	RT(Retention time)	RT Library-Compound Name	Molecular formula	Area	Area%
1	8.931	2-Chlorobenzoic acid hydrazide,4-Chlorobenzoic acid hydrazide	$C_7H_7C_1N_{20}$	29,811,840.00	0.089
2	15.661	Cyclopentaneundecanoic acid, methyl ester,Undecanoic acid, 2-methyl-	$C_{17}H_{32}O_2$, $C_{12}H_{24}O_2$	17,532,282.00	0.053
3	16.592	9,12-Octadecadienoyl chloride, (Z,Z)-,17-Octadecynoic acid	$C_{18}H_{31}C_{10}$, $C_{18}H_{32}O_2$	39,277,032.00	0.118
4	16.692	Tetradecanoic acid, 12-methyl-, methyl ester,Cyclopentaneundecanoic acid, methyl ester	$C_{16}H_{32}O_2$, $C_{17}H_{32}O_2$	14,781,189.00	0.044
5	18.461	Undec-10-ynoic acid, hexyl ester,8,11,14-Eicosatrienoic acid, (Z,Z,Z)-	$C_{17}H_{30}O_2$,$C_{20}H_{34}O_2$	34,294,676.00	0.103
6	18.961	Diisooctyl phthalate,Mono(2-ethylhexyl) phthalate	$C_{24}H_{38}O4$, $C_{16}H_{22}O_4$	565,007,936.00	1.693

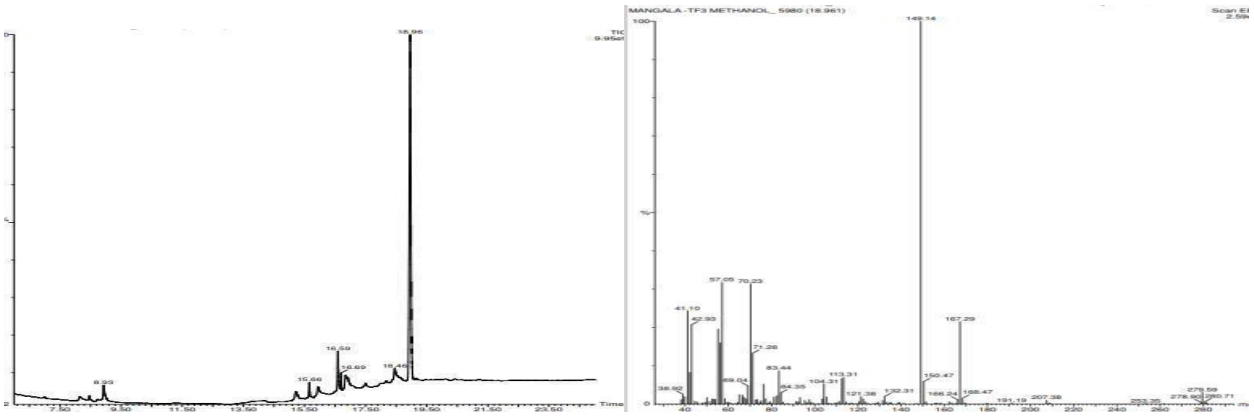


Figure 6 Gas chromatography-Mass spectrum (GC-MS) of methanol fraction of *H. griseobrunneum*

Mass analysis

The GC-MS analysis showed significantly abundant peaks, with a prominent peak observed at a retention time of 18.96 minutes showed in fig 6. This major peak was accompanied by several smaller peaks, indicating the presence of multiple components in the methanol fraction. The analysis of the 18.96 min peak was sufficient to tentatively identify the major compound present in the extract. Although minor components may have also appeared in the NMR spectrum, the technique was highly sensitive and effective in identifying the various types of hydrogen environments within the molecules. Furthermore, the presence of functional groups and specific bonds in the extract was determined using FT-IR spectroscopy, which provided distinct wavenumber values corresponding to various bond vibrations. In FT-IR, the intensity of each absorption peak is influenced by the relative electronegativity of the atoms involved in a bond, which affects the bond dipole moment and hence its infrared activity.

Fourier transform infrared spectroscopy (FT-IR) analysis:

FT-IR spectroscopy was used to identify the functional groups present in the methanol fraction of *H. griseobrunneum* TF3. The spectrum was recorded in the range of 4000–400 cm^{-1}. A sharp peak observed at 3001 cm^{-1} corresponds to the sp^2 C–H stretching vibrations of aromatic rings. The band at 2925 cm^{-1} is attributed to the C–H stretching of alkyl groups (–CH_2 and –CH_3). A distinct absorption at 2253 cm^{-1} indicates the presence of a C≡C (alkyne) stretch. A strong and sharp band at 1725 cm^{-1} represents the C=O stretching vibration of an ester functional group, characteristic of phthalate derivati4.2ves. The 1524 cm^{-1} peak corresponds to C=C stretching in aromatic rings. Multiple peaks in the 1200–1400 cm^{-1} region are associated with C–C and C–O stretching vibrations.

Additional peaks below 1000 cm^{-1} are due to C–H bending and aromatic out-of-plane vibrations. These spectral features support the presence of phthalate esters in the TF3 methanol fraction figure 7a.

Nuclear magnetic resonance spectroscopy (NMR)

^{1}H NMR analysis of the methanol fraction of *H. griseobrunneum* TF3 was performed to identify the hydrogen environments of major compounds present, without isolating individual constituents. The spectrum was interpreted using literature values and known chemical shifts characteristic of phthalate esters. In the spectrum corresponding to the major GC-MS peak at retention time 18.96 min, aromatic proton signals were observed in the 7.0–8.0 ppm range, indicating the presence of benzene ring structures. A signal at 3.4 ppm, attributed to methylene protons adjacent to ester groups, appeared to merge with ester-related protons of the compound. A multiplet at 1.26 ppm corresponded to methylene (CH_2) groups in isopropyl linkages, while a triplet at 0.90 ppm was assigned to terminal methyl (CH_3) groups. A broad signal around 2.5 ppm may represent overlapping methylene protons or residual solvent signals Figure 7b.

These spectral features are consistent with the structure of diisooctyl phthalate, the major compound tentatively identified in the *H. griseobrunneum* TF3 fraction by GC-MS.

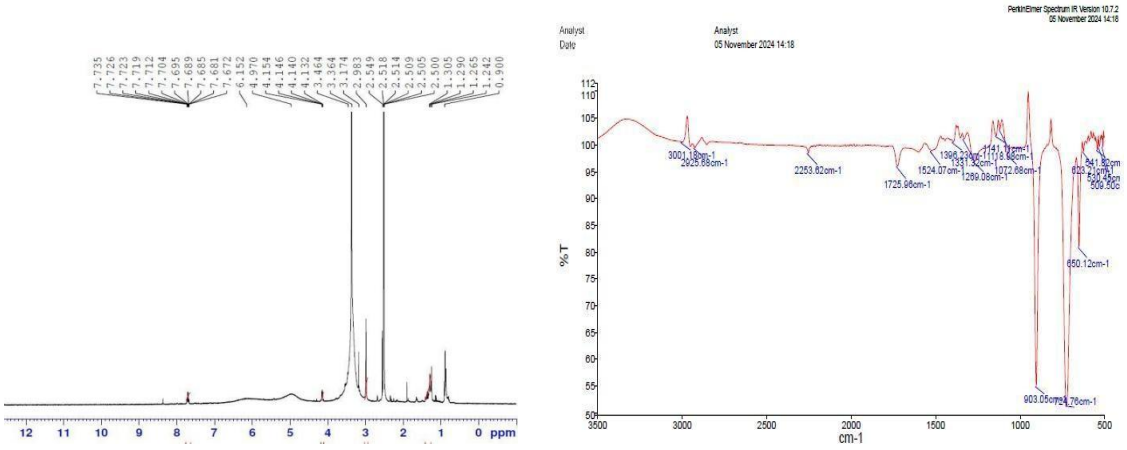


Fig .7 a. ^{1}H NMR of the compound **b. FT-IR spectrum of the compound**

Compound identified: Diisooctyl phthalate

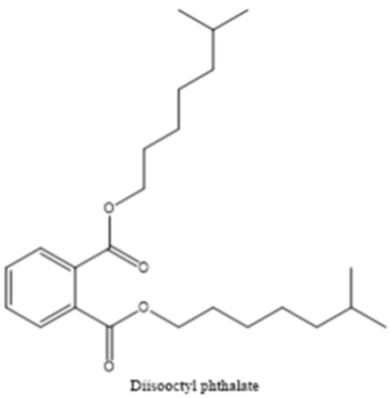


Figure 8. Diisooctyl phthalate

The methanol fraction of *H. griseobrunneum* TF3 extract contains a variety of bioactive phthalate derivatives, predominantly Diisooctyl phthalate, as confirmed by GC-MS, FT-IR, and NMR analyses. The presence of functional groups such as esters, aromatics, and alkyl chains was validated through FT-IR, while the NMR profile matched that of Diisooctyl phthalate. The identification of these compounds supports the

potential antimicrobial properties of the *H. griseobrunneum* TF3 methanol fraction, making it a promising candidate for further pharmacological evaluation.

Discussion

The present study successfully isolated and identified six endophytic fungal strains from *Thunbergia fragrans*, a plant with limited prior reports on its endophytic microbiota. These isolates, obtained from surface-sterilized leaf and stem tissues, exhibited diverse colony morphologies and growth characteristics, suggesting a rich endophytic diversity associated with this species. Molecular identification through ITS rRNA sequencing confirmed the isolates as *Talaromyces tratensis*, *Cladosporium cladosporioides*, *Hypoxylon griseobrunneum*, *Meyerozyma caribbica*, *Penicillium* sp., and *Aspergillus* sp., with GenBank accession numbers deposited for most sequences (Table 1). The diversity of endophytes isolated aligns with previous reports highlighting the ecological role of endophytic fungi in plant health and secondary metabolite production (Zhao *et al.,* 2011; Gunatilaka, 2006). Among the isolates, *Hypoxylon griseobrunneum* (TF3) was selected for further characterization due to its distinct colony morphology and superior bioactivity. Notably, TF3 exhibited strong antibacterial activity, with the highest zone of inhibition recorded against *Bacillus subtilis* (23 ± 0.18 mm), surpassing the standard antibiotic gentamicin (18 ± 0.09 mm) (Table 2). The broad-spectrum antibacterial effect of TF3 against both Gram-positive and Gram-negative bacteria is consistent with previous findings on *Hypoxylon* spp., which are known producers of bioactive secondary metabolites such as cytochalasins and phenalenones (Stadler *et al*., 2014; Kusari *et al.,* 2014).

Further, the ethyl acetate extract of TF3 displayed significant antifungal activity, particularly against *Aspergillus fumigatus* (12 ± 0.54 mm), though the inhibitory zones were generally lower than fluconazole, the reference antifungal (Table 4). The observed antifungal potential indicates the presence of diverse antimicrobial compounds, reinforcing the potential of *H. griseobrunneum* as a source of novel antifungal agents. Column chromatography of the ethyl acetate extract followed by antibacterial screening revealed that the methanol fractions exhibited the highest activity (11 mm against *B. subtilis*), while hexane fractions were inactive, indicating that the active components are likely polar (Fig. 5). These findings are consistent with studies that highlight the role of solvent polarity in extracting bioactive fungal metabolites (Wang *et al*., 2020). GC-MS analysis of the methanol fractions identified Diisooctyl phthalate as the major compound (RT: 18.961 min, 1.693% peak area), along with several other fatty acid esters and unsaturated fatty acids (Table 7; Fig. 4). Diisooctyl phthalate has been previously reported from fungal endophytes and is known for its antimicrobial and cytotoxic properties (Roy *et al*., 2014; Bousserrhine *et al*., 1999). While often regarded as a plasticizer, naturally derived phthalate esters from microbial sources have been shown to possess bioactivity, suggesting biosynthesis rather than contamination (Singh *et al*., 2012). FT-IR spectra confirmed the presence of functional groups characteristic of esters, alkenes, and aromatics, with key peaks observed at 1725 cm^{-1} (C=O stretching of esters), 3001 cm^{-1} (sp^2 C–H stretching), and 1524 cm^{-1} (C=C stretching in aromatic rings) (Fig. 7a). These findings align with the functional profile expected of phthalate derivatives. ^{1}H NMR analysis further supported the identity of Diisooctyl phthalate, with characteristic aromatic proton signals (7.0–8.0 ppm), ester methylene protons (3.4 ppm), and terminal methyl groups (0.90 ppm) (Fig. 7b). Together, the spectral data provide strong evidence for the presence of Diisooctyl phthalate as a key antimicrobial constituent in TF3 methanol fractions. The isolation of Diisooctyl phthalate from *H. griseobrunneum* underscores the potential of endophytic fungi as sources of pharmaceutically relevant secondary metabolites. While synthetic phthalates have raised environmental concerns, fungal-derived phthalates may offer bioactive scaffolds for drug development with possible structural modifications to reduce toxicity (Jia *et al*., 2021). The broad-spectrum activity of TF3, combined with its ability to produce structurally diverse compounds, makes it a strong candidate for future bioprospecting and pharmacological evaluation.

Conclusion

This study highlights the untapped potential of *Thunbergia fragrans* as a host for diverse endophytic fungi capable of producing potent antimicrobial compounds. Among them, *Hypoxylon griseobrunneum* TF3 demonstrated notable bioactivity against bacterial and fungal pathogens, attributed primarily to the presence of Diisooctyl phthalate and related metabolites. The integration of bioassays and spectroscopic analyses validates the therapeutic promise of these fungal metabolites and warrants further research into their mechanisms of action, safety profiles, and possible pharmaceutical applications.

Acknowledgments The authors gratefully acknowledge to Department of Botany, Yuvaraj's College University of Mysore, Mysore 570005, and the Department of Studies in Botany, University of Mysore, Mysore for laboratory and instrumentation facilities.

Author contributions

Mangalagowri M. S Conceptualization; Data curation; Formal analysis; Investigation; Methodology;

Resources; Software; Visualization; Roles: Writing-original draft; Review and editing.
K. Krishna: The corresponding author; Conceptualization; Validation; Investigation, formal analysis; Supervision; Roles: Review and editing.

Data availability
No datasets were generated or analysed during the current study.

Declarations
Competing interests
The authors declare no competing interests.

References

1. Akash, M., Gnanachitra, M., Balachandar, D., & Thiyageshwari, S. Eliciting Exudates Based Metabolite Analysis and Validation of Npk &Npkzn Biofertilizer Consortia Seed Coating in Maize. Penicillium crustosum Using High resolutionn Semi-preparative HPLC. *Combinatorial Chemistry & High Throughput Screening*, *27*(4), 573-583. DOI: 10.2174/1386207326666230707110651.
2. Asghari, A., Tajick Ghanbary, M. A., Bakhshi, M., & Babaeizad, V. (2023). Bioactive potential and GC-MS fingerprinting of extracts from endophytic fungi associated with seeds of some medicinal plants . *Mycologia Iranica*, *10*(1),55-67
3. Brantner, A., Pfeiffer, K. P., & Brantner, H. (1994). Applicability of diffusion methods required by the pharmacopoeias for testing antibacterial activity of natural compounds. *Die Pharmazie*, *49*(7), 512-516.
4. Bousserrhine, N., Genty, S., and Merlin, C. (1999). Biodegradation of phthalic acid esters by microorganisms. *Environmental Microbiology*, 1(3), 207–212.
5. El-Sayed, O., Asker, M., Shash, S., & Hamed, S. (2015). Isolation, Structure elucidation and Biological Activity of Di- (2-ethylhexyl) phthalate Produced by Penicillium janthinellum 62. *International Journal of ChemTech Research*, *8*, 974–4290.
6. Faeth, S. H., & Fagan, W. F. (2002). Fungal endophytes: common host plant symbionts but uncommon mutualists. *Integrative and Comparative Biology*, *42*(2), 360-368 https://doi.org/10.1093/icb/42.2.3608–14. https://doi.org/10.1016/j.biocontrol.2014.10.004
7. Giang, T. T. H., Quan, N. D., Linh, D. A., Lan, N. N., Lien, N. T. K., & Hoang, N. H. (2021). Isolation and Identification Of Endophytic Fungi From Catharanthus roseus and Scutallaria barbata. *Journal of Biology/TẠp chí Sinh HỌc*, *43*(2).
8. Gunatilaka, A. A. L. (2006). Natural products from plant-associated microorganisms: Distribution, structural diversity, bioactivity, and implications of their occurrence. *Journal of Natural Products*, 69(3), 509–526.
9. Huang, L., Zhu, X., Zhou, S., Cheng, Z., Shi, K., Zhang, C., & Shao, H. (2021). Phthalic Acid Esters: Natural Sources and Biological Activities. *Toxins*, *13*(7), Article 7. https://doi.org/10.3390/toxins13070495
10. Jia, X., Liu, H., Pan, C., and Liu, X. (2021). Biosynthesis of phthalate esters: Current status and future perspectives. *Applied Microbiology and Biotechnology*, 105, 1275–1287.
11. Kusari, S., Hertweck, C., & Spiteller, M. (2014). Chemical ecology of endophytic fungi: Origins of secondary metabolites. *Chemical Biology*, 21(9), 1103–1112.
12. Lotfy, M. M., Hassan, H. M., Hetta, M. H., El-Gendy, A. O., & Mohammed, R. (2018). Di-(2-ethylhexyl) Phthalate, a major bioactive metabolite with antimicrobial and cytotoxic activity isolated from River Nile derived fungus *Aspergillus awamori*. *Beni-Suef University Journal of Basic and Applied Sciences*, *7*(3), 263–269. https://doi.org/10.1016/j.bjbas.2018.02.002
13. Lykholat, Y. V., Khromykh, N. O., Didur, O. O., Drehval, O. A., Sklyar, T. V., & Anishchenko, A. O. (2021). Chaenomeles speciosa fruit endophytic fungi isolation and characterization of their antimicrobial activity and the secondary metabolites composition. *Beni-Suef University Journal of Basic and Applied Sciences*, *10*(1), 83. https://doi.org/10.1186/s43088-021-00171-2
14. Mahabaleshwara, K., Chandrasekhar, N., & Govindappa, M. (2016). Phytochemical investigations of methanol leaf extracts of Randia spinosa using column chromatography, HPTLC and GC-MS. *Nat Prod Chem Res*, *4*(202), doi:10.4172/2329-6836.1000202
15. Nuraini, F. R., Setyaningsih, R., & Susilowati, A. (2023). Antibacterial activity of bioactive compound produced by endophytic fungi isolated from Mangifera casturi Kosterm endemic plant from South Kalimantan, Indonesia. *Indonesian Journal of Biotechnology*, *28*(2),77-85.
16. Rodrigues, K. F., Hesse, M., & Werner, C. (2000). Antimicrobial activities of secondary metabolites produced by endophytic fungi from Spondias mombin. *Journal of Basic Microbiology: An International Journal on Biochemistry, Physiology, Genetics, Morphology, and Ecology of Microorganisms*, *40*(4),261-267.
17. Roy, R. N., Laskar, S., and Sen, S. K. (2014). Di-(2-ethylhexyl) phthalate: A metabolite of *Streptomyces albidoflavus* with antibacterial properties. *Journal of Applied Microbiology*, 116(3), 703–711.
18. Singh, A., Singh, S., and Khare, P. (2012). Isolation of a phthalate derivative from a fungal

endophyte with potential antimicrobial activity. *Current Science*, 102(2), 297–300.
19. Stadler, M., Læssøe, T., Fournier, J., Decock, C., Schmieschek, B., Tichy, H. V., and Peršoh, D. (2014). A polyphasic taxonomy of *Hypoxylon* species. *Studies in Mycology*, 77,1–144.
20. Singh, A., Jones, S., Ganapathysubramanian, B., Sarkar, S., Mueller, D., Sandhu, K., & Nagasubramanian, K. (2021). Challenges and opportunities in machine-augmented plant stress phenotyping. *Trends in Plant Science*, *26*(1),53-69.
21. Schulz, B., Boyle, C., Draeger, S., Römmert, A. K., & Krohn, K. (2002). Endophytic fungi: a source of novel biologically active secondary metabolites. *Mycological research*, *106*(9), 996- 1004. https://doi.org/10.1017/S0953756202006342
22. Strobel, G., Daisy, B., Castillo, U., & Harper, J. (2004). Natural products from endophytic microorganisms. *Journal of Natural products*, *67*(2), 257-268.
23. Sun, Z.-L., Zhang, M., Zhang, J.-F., & Feng, J. (2011). Antifungal and cytotoxic activities of the secondary metabolites from endophytic fungus Massrison sp. *Phytomedicine*, *18*(10), 859–862. https://doi.org/10.1016/j.phymed.2011.01.019
24. Tamura, K., Nei, M., & Kumar, S. (2004). Prospects for inferring very large phylogenies by using the neighbor-joining method. *Proceedings of the National Academy of Sciences of the United States of America*, *101*(30), 11030–11035. https://doi.org/10.1073/pnas.0404206101.
25. Thirawatthana, P., Palaga, T., Jittra, P., Whalley, A., & Sihanonth, P. (2013). Antimicrobial and anticancer activities of endophytic fungi from Mitrajyna javanica Koord and Val. *African Journal of Microbiology Research*, *7*, 5565–5572. https://doi.org/10.5897/AJMR12.2352
26. Tuyen, D. T., Trung, N. T., Thao, N. T., Le Thanh, N. S., Dai Nguyen, N. P., Anh Tuyet, N. T., Cuong, N. T., Chan, S. S., Khoo, K. S., & Show, P. L. (2023). Antifungal activity of secondary metabolites purified from *Bacillus subtilis* isolated in Vietnam and evaluated on *in vitro* and *in vivo* models. *International Biodeterioration & Biodegradation*, *179*, 105558. https://doi.org/10.1016/j.ibiod.2022.105558
27. Wilson, D. (1995). Endophyte: the evolution of a term, and clarification of its use and definition. *Oikos*, 274-276. https://doi.org/ 10.2307/ 3545919
28. Wang, Y., Xu, Y., Zhang, X., and Wang, J. (2020). Solvent-dependent bioactive compound extraction from endophytes: A review. *Journal of Applied Microbiology*, 129(4), 1030–1045.
29. White, T. J., Bruns, T., Lee, S., & Taylor, J. (1990). Amplification and direct sequencing of fungal ribosomal RNA genes for phylogenetics. In M. A. Innis, D. H. Gelfand, J. J. Sninsky, and T. J. White (Eds.), *PCR protocols: A guide to methods and applications* (pp. 315–322).
30. Zhao, J., Shan, T., Mou, Y., and Zhou, L. (2011). Plant-derived bioactive compounds produced by endophytic fungi. *Mini Reviews in Medicinal Chemistry*, 11(2), 159–168.
31. Zardoya, R. (2021). Quest for the best evolutionary model. *Journal of Molecular Evolution*, *89*(3), 146-150. https://doi.org/10.1007/s00239-020-09992-8